Subseasonal Deterministic Prediction Skill of Low-Level Geopotential Height Affecting Southern Africa

CHRISTIEN J. ENGELBRECHT,[a,b] STEVEN PHAKULA,[a,b] WILLEM A. LANDMAN,[b] AND FRANCOIS A. ENGELBRECHT[c]

[a] *South African Weather Service, Pretoria, South Africa*
[b] *Department of Geography, Geoinformatics and Meteorology, University of Pretoria, Pretoria, South Africa*
[c] *Global Change Institute, University of the Witwatersrand, Johannesburg, South Africa*

(Manuscript received 14 January 2020, in final form 24 August 2020)

ABSTRACT: The NCEP CFSv2 and ECMWF hindcasts are used to explore the deterministic subseasonal predictability of the 850-hPa circulation of a large domain over the Atlantic and Indian Oceans that is relevant to the weather and climate of the southern African region. For NCEP CFSv2, 12 years of hindcasts, starting on 1 January 1999 and initialized daily for four ensemble members up to 31 December 2010 are verified against ERA-Interim reanalysis data. For ECMWF, 20 years of hindcasts (1995–2014), initialized once a month for all the months of the year are employed in a parallel analysis to investigate the predictability of the 850-hPa circulation. The ensemble mean for 7-day moving averages is used to assess the prediction skill for all the start dates in each month of the year, with a focus on the start dates in each month that are representative of the week-3 and week-4 hindcasts. The correlation between the anomaly patterns over the study domain shows skill over persistence up into the week-3 hindcasts for some months. The spatial distribution of the correlation between the anomaly patterns show skill over persistence to notably reduce over the domain by week 3. A prominent area where prediction skill survives the longest, occur over central South America and the adjacent Atlantic Ocean.

KEYWORDS: Climate prediction; Ensembles; Forecast verification/skill; Hindcasts; Operational forecasting; Seasonal forecasting

1. Introduction

Subseasonal prediction, defined as forecasts with a lead time of more than two weeks but less than one season (Vitart et al. 2017) is globally becoming more in demand (White et al. 2017). Skillful subseasonal forecasts have the potential to provide valuable guidance in the decision-making process across many sectors of which disaster management, water management, and agriculture are keys within the southern African context. The climate over southern Africa is highly variable (Mason and Jury 1997) and extreme weather events are not uncommon (Fauchereau et al. 2003). These extremes, which can have devastating economic and societal impacts, include droughts (e.g., Joubert et al. 1996; Rouault and Richard 2005; Sousa et al. 2018), floods (e.g., Reason and Keibel 2004; Hart et al. 2010), severe convective storms (Blamey and Reason 2009), heat waves (e.g., Lyon 2009) and wildfires (e.g., Kraaij et al. 2018). Recent occurrences of extreme weather events in southern Africa include the heat waves of the 2015–16 austral summer season, in particular the heat wave during the first week of January 2016, the Knysna fires that occurred at the end of October 2018, Tropical Cyclone Idai that made landfall over Mozambique in March 2019, and the Durban floods of April 2019. These particular extreme weather events did not only have economic and societal impact, but also resulted in the loss of life. Even though these events were forecast accurately on the short-range time scale, that is, for a few days in advance, more efficient preparedness require skillful forecasts at sufficiently long lead times for timeous decision-making. That is, reliable forecasts at subseasonal time scales indicating a high likelihood of extreme events to occur can result in an enhanced level of preparedness by the time of actual occurrence.

Subseasonal prediction skill remains largely unexplored for the southern African region with only a few studies that focused on subseasonal temperature prediction (Engelbrecht 2017; Phakula et al. 2020), whereas this time scale is being increasingly explored over other parts of the world (e.g., Tian et al. 2017; Batté et al. 2018; Osman and Alvarez 2018). For some regions there are indications that skillful subseasonal prediction is feasible, largely through the large-scale circulation modes such as the Madden–Julian oscillation (MJO) (e.g., Mundhenk et al. 2018) and El Niño–Southern Oscillation (ENSO) (e.g., White et al. 2014), which act as sources of predictability. Improved representation of initial conditions and initialization procedures (e.g., Seo et al. 2019) have also proven to be potential sources of enhanced subseasonal predictive skill. Over southern Africa, the state of ENSO is the main source of seasonal predictability (e.g., Landman and Beraki 2012) and has also been associated with skill in predicting intraseasonal circulation characteristics over the all-year rainfall region of South Africa (Engelbrecht and Landman 2016; Engelbrecht et al. 2017). In addition, skillful prediction of seasonal rainfall characteristics including onset over South Africa have also been demonstrated (Phakula et al. 2018). Predictability at the seasonal time scale over southern Africa is mostly found over the summer rainfall region and during the

Supplemental information related to this paper is available at the Journals Online website: https://doi.org/10.1175/WAF-D-20-0008.s1.

Corresponding author: Christien J. Engelbrecht, christien.engelbrecht@weathersa.co.za

DOI: 10.1175/WAF-D-20-0008.1

austral midsummer period (Landman and Beraki 2012). Marginal seasonal prediction skill has also been demonstrated for the austral midwinter season over the winter rainfall region of South Africa (Archer et al. 2019), a region where the climate is dictated by the meridional movement of the westerly wind regime and is climatologically distinctly different from the predominantly summer rainfall regions of South Africa.

As subseasonal prediction is in its infancy for the southern African region, we focus here only on the predictability of circulation for a domain over which the tropical and extratropical weather systems that are relevant to southern African weather and climate co-occur. A main objective of this study is to determine the lead time of deterministic subseasonal predictive skill of the low-level circulation as described by the 850-hPa geopotential height, and to analyze whether a seasonal cycle exists in subseasonal predictive skill. The subseasonal predictions of two state-of-the-art forecast systems are used for this purpose. The methodology followed is presented in section 2, results are shown and discussed in section 3, and conclusions are drawn in section 4.

2. Data and methods

a. Data

This study is based on hindcasts of 850-hPa geopotential height generated by two state-of-the-art subseasonal prediction systems, namely the National Centers for Environmental Prediction (NCEP) Climate Forecast System version 2 (CFSv2) and those of the European Centre for Medium-Range Weather Forecasts (ECMWF). The hindcasts of 850-hPa geopotential height produced by NCEP CFSv2 and ECMWF were obtained from the database of the S2S Prediction project, via the data portal administered by the ECMWF (http://apps.ecmwf.int/datasets/data/s2s). Both forecast systems rely on fully coupled atmosphere–ocean–land–sea ice models for dynamic seasonal prediction. Model initial conditions are obtained from the Climate Forecast System Reanalysis (CFSR) for NCEP CFSv2 and an ensemble of four forecasts is produced each day by initialization at 6-hourly intervals (Saha et al. 2014). The NCEP forecasts, for both the hindcasts and real-time forecasts, are generated from a fixed model version and is archived on a common 1.5° horizontal resolution for the period of 1999–2010. The ECMWF hindcasts (11 ensemble members) are available on the same horizonal resolution for the period 1995–2014 via the ECMWF data portal.

In this study, the ERA-Interim reanalysis (Dee et al. 2011), also available on a 1.5° horizontal resolution through the ECMWF data portal, is used as observational reference for the 850-hPa geopotential height forecasts. Both the NCEP CFSv2 and ECMWF forecast fields are instantaneous values at 0000 UTC and the corresponding time of the ERA-Interim reanalysis fields are used in the verification process of which a detailed discussion follows below.

b. Verification design

Extreme weather events over southern Africa are associated with distinct low-level circulation features (e.g., Singleton and Reason 2007), while low-level circulation fields have been shown to be a good predictor for seasonal climate anomalies (Landman and Goddard 2002) as well as to describe the distribution of weather patterns within a season (Engelbrecht et al. 2017). Here, consideration is given to the topography of southern Africa, rendering 850 hPa as the most suitable standard pressure level in terms of depicting near-surface circulation. The domain over which the predictability of low-level circulation is assessed is also important, as the weather and climate over southern Africa are influenced by tropical (e.g., Pascale et al. 2019; Malherbe et al. 2012) and midlatitude (e.g., Reason and Rouault 2005) weather systems, as well as by the interaction of weather systems from these two distinct circulation regimes (e.g., Hart et al. 2010). The domain over which forecast circulation anomalies are evaluated is thus chosen to include the important geographical regions from where weather systems develop and propagate to influence the southern African region. These include the regions of maximum cyclogenesis over the southwestern Atlantic Ocean (Simmonds and Keay 2000) from where frontal systems move eastward, the southwest Indian Ocean from where tropical weather systems move westward toward the subcontinent to make landfall (Malherbe et al. 2012) as well as continental Africa where the Angola low (e.g., Pascale et al. 2019) and the Botswana high (e.g., Driver and Reason 2017) can result in circulation anomalies that are associated with extreme or high-impact weather over southern Africa. The domain used in this study is thus bounded by 60°–10.5°S, 79.5°W–79.5°E and capture all the weather systems described above as well as the subtropical high pressure belt that extend ridging highs toward the subcontinent (e.g., Engelbrecht and Landman 2016).

In this paper, a deterministic assessment is performed and hence an ensemble average is calculated for each forecast system prior to the calculation of the verification metrics. The approach of dividing each start date's integration period into weekly segments (e.g., Mastrangelo and Malguzzi 2019) is followed. The models' skill in the prediction of weekly moving averaged geopotential height anomalies at 850 hPa are assessed using each start date (date of model initialization) within each of the calendar months from January to December. For the NCEP CFSv2 forecasts daily start dates are available with four ensemble members per day over the period 1999–2010. For 31-day (30-day) months, there are thus 372 (360) start dates (Fig. 1). There are no leap years occurring in the forecasts, so that the month of February always has 336 start dates. The 45-day runs of the CFSv2 hindcasts are available from the S2S database (Vitart et al. 2017) and the first 28 days of each start date have been obtained for use in this study. A 28-day forecast is used for each start date within each of the calendar months toward assessing the subseasonal predictability of weekly moving averaged circulation anomalies and the evolution of the synoptic-scale error. The 28-day integration period for each start date translates to 22 leads per start date when weekly moving averages are calculated (see Fig. 1). The ECMWF hindcasts are similarly structured. The analysis relies on four ensemble members generated for a start date closest to the beginning of the month.

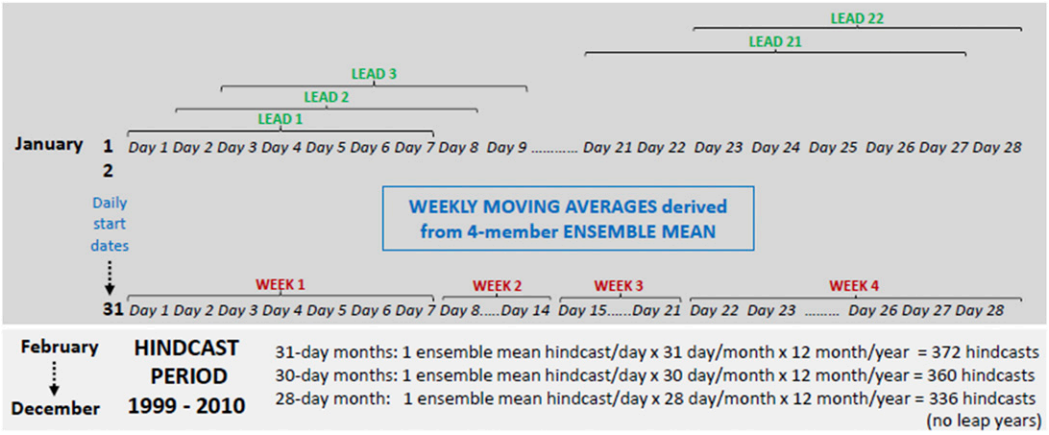

FIG. 1. Schematic of the experimental design used for the deterministic assessment of skill in predicting the 850-hPa circulation anomalies by using the NCEP GFSv2 hindcasts. Weekly moving averages are calculated over a 28-day integration period for every start date, translating to different 22 lead times being considered for each start date. Lead 1, lead 8, lead 15, and lead 22 are equivalent to a week-1, week-2, week-3, and week-4 forecasts, respectively.

A widely used verification metric for deterministic forecasts is the anomaly correlation coefficient (ACC). Here, the ACC is used to assess the skill in predicting weekly averaged low-level circulation across lead times ranging from 1 to 22 days for all the start dates and is presented as a spatial average over the study domain (60°–10.5°S, 79.5°W–79.5°E) for the respective calendar months. That is, for each calendar month the ACCs are averaged for hindcasts of the same lead time obtained during that month, toward obtaining insight in the behavior of error growth for forecasts of different lead times issued during that calendar month. The anomalies in the computation of the ACC is relative to the weekly hindcast and reanalysis climatologies and are a function of the lead time and start date, respectively. Skill is determined relative to the corresponding persistence forecasts, where persistence is defined as the observation of the weekly mean circulation calculated from day $(d - N - 6)$ to day $(d + N - 1)$ to be used as the prediction of the weekly mean circulation calculated from day $(d + N)$ to day $(d + N + 6)$. Here N, for the set of hindcasts considered, assumes values from 1 to 22.

To investigate the spatial attributes of the model skill in predicting weekly circulation anomalies across the 22 lead times for all the start dates in a particular calendar month, the correlation of anomalies (AC) between the ensemble mean hindcast and the corresponding reanalysis fields are determined at each grid point over the domain of interest (60°–10.5°S, 79.5°W–79.5°E). As before, for a given lead time the hindcasts obtained over the period of 1999–2010 are averaged in terms of the correlation to gain insight in the time evolution of hindcast skill. The weekly moving average anomalies (for both the hindcasts and the ERA-Interim reanalysis data) are in this case relative to the corresponding domain average (60°–10.5°S, 79.5°W–79.5°E) of 850-hPa geopotential heights. This method of calculating anomaly fields derives spatial gradient fields which are associated with the movement of weather systems. Skill is determined relative to the corresponding persistence forecasts, where the persistence forecasts are defined exactly as in the calculation of the ACC.

3. Results and discussion

The daily temporal resolution of output of the two forecast systems enables the verification of predictive skill of weakly means continuous from lead 1 (week 1) through to lead 22 (week 4) (see Fig. 1). This effectively makes feasible an analysis of predictive skill from the short-range weather time scale through to the unexplored (over southern Africa) subseasonal time scale. As the domain over which the prediction skill of low-level circulation is assessed range from the tropical latitudes deep into the midlatitudes, it is to be expected that the skill will be a function of latitude and the time of year in response to different sources of predictability and their seasonality. In particular, it is known that ENSO is a key source of seasonal prediction over southern Africa during midsummer (Landman and Beraki 2012) and this may translate to skill at the subseasonal time scale during this time of the year that is so important for agriculture, water security and disaster management. To investigate the seasonal cycle of prediction skill, a first evaluation is performed through the averaged ACC over the domain under investigation, thus measuring the correlation between forecast and reanalysis anomalies over the domain (Fig. 2 and Table 1). This evaluation of the prediction skill averaged over the domain is expanded to an evaluation that considers the spatial attributes of the prediction skill (Figs. 3–6).

The ACC for forecasts of 7-day moving averages is calculated separately for each month and for lead times of 1–22 days. The results obtained are presented as averages over the domain being studied for each of the twelve calendar months. The results obtained for the NCEP CFSv2 are shown in Fig. 2. Up until a lead time of about 5 days, the weekly averaged circulation anomalies show comparable levels of ACC between the different months, where after the gradual divergence in the

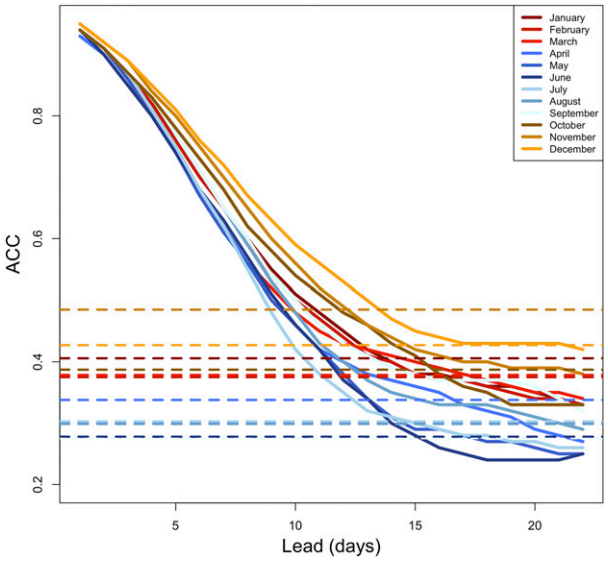

FIG. 2. Anomaly correlation coefficients for different calendar months over the hindcast period of 1999–2010 for the NCEP GFSv2 hindcasts of 7-day moving averages of the 850-hPa geopotential height anomalies obtained at lead times ranging from 1 to 22 days. All the start dates within a month are considered in setting up the average evolution of the ACC. The stippled lines indicate the ACC for the various months associated with the persistence forecasts (using the observations of week $N - 1$ as a forecast for week N).

ACCs obtained for the various months systematically increases. The highest ACCs are generally achieved for the summer months, with the late autumn and midwinter months (May–July) having the lowest ACCs. This pattern of relatively higher ACCs during the summer start date months occur consistently over all the lead times. This finding differs from that of Mastrangelo and Malguzzi (2019) who considered the ACCs for 500-hPa circulation over the extratropical regions of both hemispheres (poleward of 20°S and 20°N) and found the highest skill during the respective cold months of both hemispheres over a 2-yr-long verification period. This difference in the seasonal cycle of ACC is very likely due to the extratropical domain focus of Mastrangelo and Malguzzi (2019) versus the South Atlantic–South Indian Ocean domain focus of the analysis presented here. The behavior of the ACC across the lead times during all the months reveal a relatively steep negative gradient to about a lead of 10 days, after which the gradient flattens out during weeks 3 and 4 with it being zero for some of the months. This may suggest that at these longer lead times the hindcasts are starting to relax to climatology, that is, the day to day simulated weather patterns are occurring largely independent of the model initial conditions. The increased rate in the loss of skill as a function of lead time between week 2 and week 3 as shown here, has also been found in an evaluation of skill in forecasting weekly averaged 500-hPa heights (Mastrangelo and Malguzzi 2019). For weeks 3 and 4, the December start date forecasts have the highest ACC, while the June start date forecasts have the lowest ACC (ACCs of 0.4 versus 0.2, respectively). Compared to the persistence forecasts, the December start date forecasts are skillful for most lead times with the June start date forecasts that remain skillful up to a lead of about 15 days (~week 3). Most of the start date months are skillful relative to persistence forecasts for leads between 15 and 17 days. Forecasts with start dates in September are also skillful over persistence for all lead times considered in this study. The August forecasts are skillful up to about a lead of 20 days (~week 4, similar to the September and December hindcasts). A surprising result, is the November start date forecasts that are only skillful relative to persistence up to a lead of 12 days, making the November forecasts the least skillful of all the months. The November start date forecasts have the second highest ACC over almost all the lead times; however, the ACC of the persistence forecasts for November is the highest for all the months (Fig. 2), explaining the weak performance of the November forecasts in terms of skill over persistence. In general, for the area under consideration, some deterministic prediction skill over persistence exists up to week 3, but this has largely been extinguished for most months by week 4.

TABLE 1. Lead time in days for each calendar month of NCEP CFSv2 and ECMWF for which the ACC is higher than 0.5.

	NCEP CFSv2	ECMWF
January	10	8
February	10	10
March	9	7
April	9	6
May	9	9
June	9	8
July	8	7
August	9	9
September	10	11
October	11	9
November	11	11
December	13	8

To explore the robustness of the results depicted in Fig. 2, Table 1 draws a comparison of hindcast skill in predicting 7-day moving averages of circulation across independently configured forecast systems. Table 1 shows the lead time (days) for which the ACC remains higher than 0.5, for the NCEP ensemble means constructed from hindcasts with daily start dates (Fig. 1) and 4 ensemble members per day and the ECMWF ensemble means constructed from a single start date per month having 4 ensemble members. In general, for both NCEP CFSv2 and ECMWF despite the differential formulation of the verification design, hindcast skill is higher for the summer compared to the winter months (Table 1). For the NCEP CFSv2 system the ACC when averaged across all calendar months remains higher than 0.5 for a lead time 0f 9.83 days, while the smaller ECMWF ensemble yields a value of 8.58 days. When the NCEP ensemble is reduced in start dates to closely resembles the ECMWF ensemble used here, the corresponding ACC value obtained is 7.5.

The spatial distribution of the correlation between the anomaly patterns of the ensemble mean and the reanalysis fields, averaged over the start dates per calendar month (for

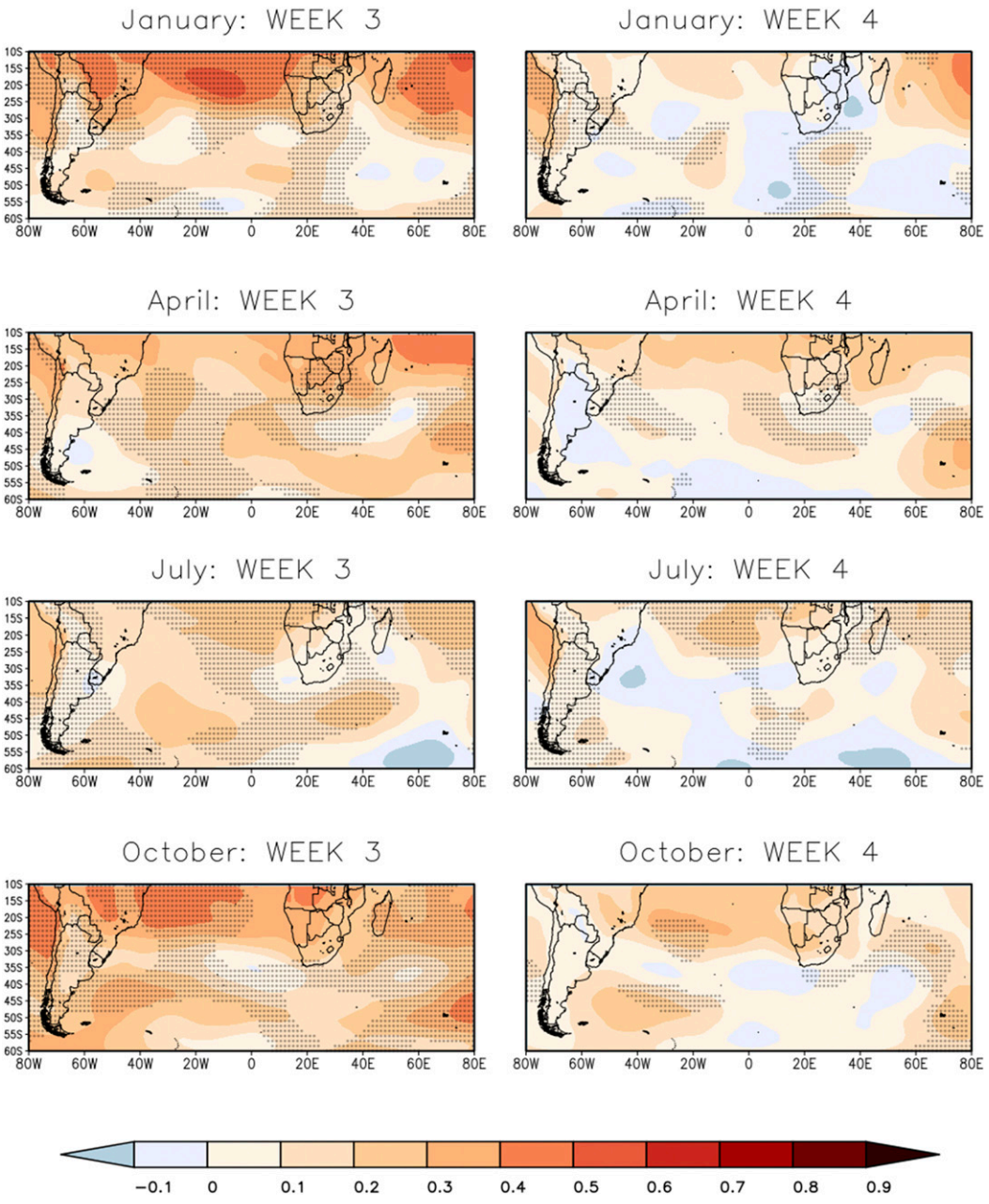

FIG. 3. Weekly mean 850-hPa geopotential height correlation between NCEP CFSv2 forecasts and ERA-Interim for lead time in days corresponding to weeks 3 and 4 for January, April, July, and October. Crosses indicate where the forecasts outscore the persistence forecast.

January, April, July, and October) for weeks 3 and 4, are shown in Figs. 3 and 5 for NCEP CFSv2 and ECMWF, respectively. Only the middle months of each of the four seasons are shown. The corresponding analysis for the remaining months of the various seasons are available in the supplementary material section, as Figs. S1 and S2 in the online supplemental material). For the NCEP CFSv2 January start dates, ACs are the highest in the tropics for the week 3 hindcasts (Fig. 3), while a second band of relatively high ACs exist in a zonal band in the mid-latitudes, stretching from the southern tip of South America eastward over the Southern Ocean, to the south of South Africa. ACs are relatively smaller in the subtropics and in the high latitudes. The forecasts are skillful relative to persistence in the tropics, except in the Mozambique Channel east of South Africa. Zonal bands of skill stretch from the tropics southward into the northern parts of South America, and similarly to South Africa and from there farther southward into the Southern Ocean. Otherwise, over large parts of the Southern Ocean the hindcasts are not skillful. These areas are where the westerlies prevail and standard deviations in the geopotential

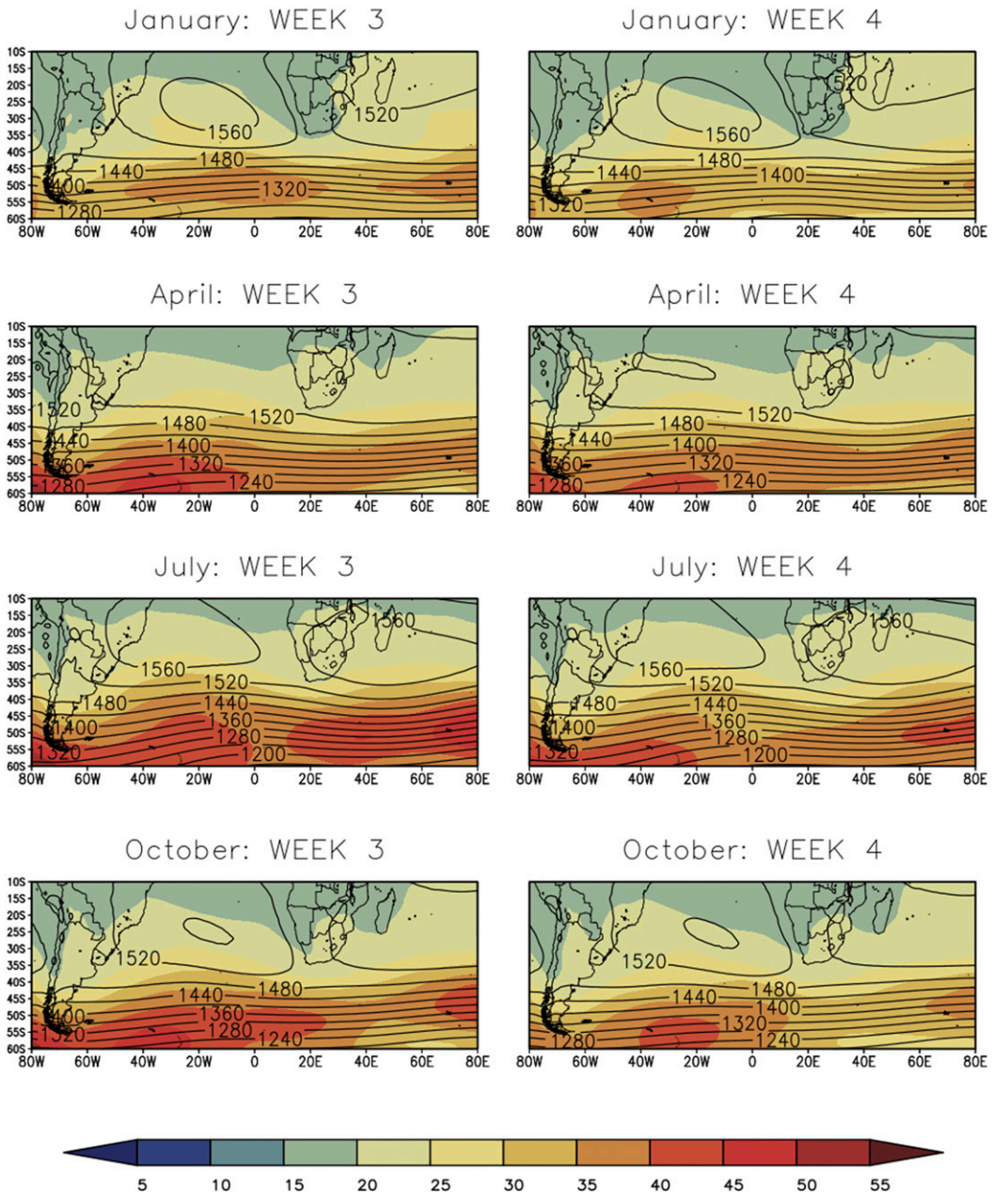

FIG. 4. NCEP GFSv2 weekly mean climate of the 850-hPa geopotential height (contours) and the standard deviation (shaded colors) of the hindcasts corresponding to weeks 3 and 4 for January, April, July, and October.

height hindcasts are the largest (Fig. 4). Consistently, Fig. 2 indicates that for the domain as a whole skill over persistence has been largely lost by week 3 of the hindcasts. By week 4 skill over persistence has also been lost in the tropics. Interestingly, skill still persists over much of central South America and in a zonal band stretching from the southern tip of southern Africa into the Southern Ocean. For ECMWF, the spatial distribution of ACs across the domain are similar to that of NCEP for week 3. A notable difference for week 4 between NCEP and ECMWF is the skill over persistence that remains over large parts of the tropics for the ECMWF hindcasts.

The week-3 NCEP hindcasts for February and March (Figs. S1 and S2) are similarly skillful in the tropics. The hindcasts are also skillful over parts of South America including the monsoon region and off the coast over the Atlantic Ocean, as well as over parts of the Indian Ocean east of southern Africa eastward into the Southern Ocean. Figure 2 consistently indicates that by week 3 the February and March hindcasts are only marginally skillful over persistence over the domain as a whole. By week 4 skill over persistence has also been lost in the tropics. It is interestingly maintained in the February hindcasts in a band stretching from the Indian Ocean

east of southern Africa southward into the Southern Ocean as well as over parts of the southwestern Atlantic Ocean neighboring South America in the February and March hindcasts. The ECMWF hindcasts qualitatively correspond to those of NCEP in terms of the spatial patterns of skill for weeks 3 and 4, indicating the robustness of the findings. Of particular interest in the ECMWF hindcasts is the area of relatively high ACs and predictive skill that exist east of the southern tip of South America in the South Atlantic Ocean. This is also a feature of the NCEP hindcast skill for these months. The areas of skill that stretch eastward of this region in both forecast systems qualitatively suggest that the models derive skill from the initial conditions of midlatitude systems, that is, the downstream propagation of the systems can be predicted with relatively high accuracy in this region into week 3. Cyclogenesis over the southern tip of South America may be particularly important in this regard (Simmonds and Keay 2000).

The ACs for the NCEP April (Fig. 3) hindcasts display some qualitative differences for week 3, compared to the January–March patterns. ACs are still the highest in the tropics, but over the northernmost part of the domain skill over persistence has been lost. Skill only marginally exists for the domain as a whole (Fig. 2), while Fig. 3 reveals that the regions with skill are located largely over the South Atlantic Ocean and over southern Africa. Only small pockets of skill persist in these regions for week 4. In the ECMWF hindcasts, skill is similarly lost for weeks 3 and 4 in April in the tropics compared to the preceding austral summer months. This further affirms the robustness of the findings indicating that the same dynamics and physics are at work as the main determinants of skill across independently formulated hindcasts systems. The ECMWF hindcasts show comparatively high skill east of the southern tip of South America for week 3. This may be indicative of model initialization capturing weather systems that pass through the Drake Passage or that that are generated in the Weddell Sea and then move northeastwards (Taljaard 1967). The importance of accurate initialization and forecasts in this region are emphasized by the high standard deviations occurring in the week-3 hindcasts of both hindcast systems (Fig. 6).

For the period of May and June (Fig. S1), through to July (Fig. 3) and August (Fig. S1), it is important to consider the accuracy in terms of the midlatitude circulation that brings winter rainfall to the southern tip of southern Africa. The winter rainfall region of South Africa receives most of its rainfall through cold fronts, embedded in the westerly wind regime but that have moved sufficiently northward while progressing eastward. During May, for week 3 of the NCEP hindcasts, skill is absent over most of the southern Atlantic Ocean over the parts where the storm tracks occur. However, skill persists into week 4 over the subcontinent and the adjacent Indian Ocean regions as well as the Atlantic Ocean to the west. During June, an interesting local maximum skill area exists at about 35°S and 20°W over the Southern Ocean. This is a region where a relatively high density of cyclogenesis occurs (Simmonds and Keay 2000) and cyclone centers exist (Taljaard 1967). By week 4 that skill over persistence has eroded. During July (Fig. 3), relatively high skill exists over large parts of the Atlantic Ocean, with a maximum over the southern central parts of this ocean, occurring in an area characterized by relatively deep cyclones throughout the year (Simmonds and Keay 2000), to the east of the climatological trough (Fig. 4). In August, an increase in ACs occur over the South America Monsoon region relative to the preceding winter months. The most striking feature in the ECMWF hindcasts is the prominence of the area of high ACs and skill that exist at about 35°S and 20°W over the Southern Ocean in the week-3 hindcasts for all of the months from May through to August. Similar to the NCEP skill for week 3, this suggests some robustness of the findings across the different hindcast systems. It may be noted that this region in the Southern Ocean corresponds to a trough like pattern of high standard deviations for the week-3 and week-4 hindcasts of both hindcast systems (Figs. 4 and 6, Figs. S3 and S4).

ACs for the NCEP hindcasts are relatively high in the tropics for September (Fig. S1), October (Fig. 3), and November–December (Fig. S1) compared to the cooler May–August period for both weeks 3 and 4. However, for both September and October the hindcasts are generally not skillful in the tropics, except in the tropical North Atlantic east of South America. The hindcasts are skillful in the mid- and high latitudes over the Southern Ocean for September, and over the midlatitude Southern Ocean for October. For September skill over persistence is maintained over southern Africa for both weeks 3 and 4, but it is lost over this region in October already by week 3. An important feature of hindcasts for November and December is that skill is maintained over large portions of the subtropics including southern Africa for week 3, and this persists over southern Africa in week 4 of the November hindcasts. In the ECMWF hindcasts, skill is similarly limited in the tropics for the months of September (Fig. S2) and October (Fig. 3), the most notable exception being the skill that exists over the South American monsoon region in the week-3 hindcasts for September. The ECMWF hindcasts are generally skillful in September of the high latitudes of the Southern Ocean, but this skill is diminished by week 4. Another similarity between the NCEP and ECMWF hindcasts is the skill that exists over southern Africa in the week-3 and week-4 hindcasts for September, but with skill being absent over this region in the corresponding hindcasts. The ECMWF hindcasts are similarly also skillful over southern Africa for week 3 for both November and December, but with diminished skill in week 4 (Figs. S1 and S2).

Given the well know peak in seasonal forecast skill over southern Africa in summer during positive and negative phases of ENSO, the question may be posed whether the same result holds at subseasonal time scales. To investigate this possibility the week-3 and week-4 hindcasts of December, January, and February were divided into years of ENSO events as opposed to neutral events. The ACC calculated for the study domain as well as for selected subregions (southern Africa, South America and the southwest Atlantic Ocean) revealed no statistically significant differences in the skill of the subseasonal forecasts for ENSO versus non-ENSO years. This may suggest, that the S2S skill present in the hindcasts

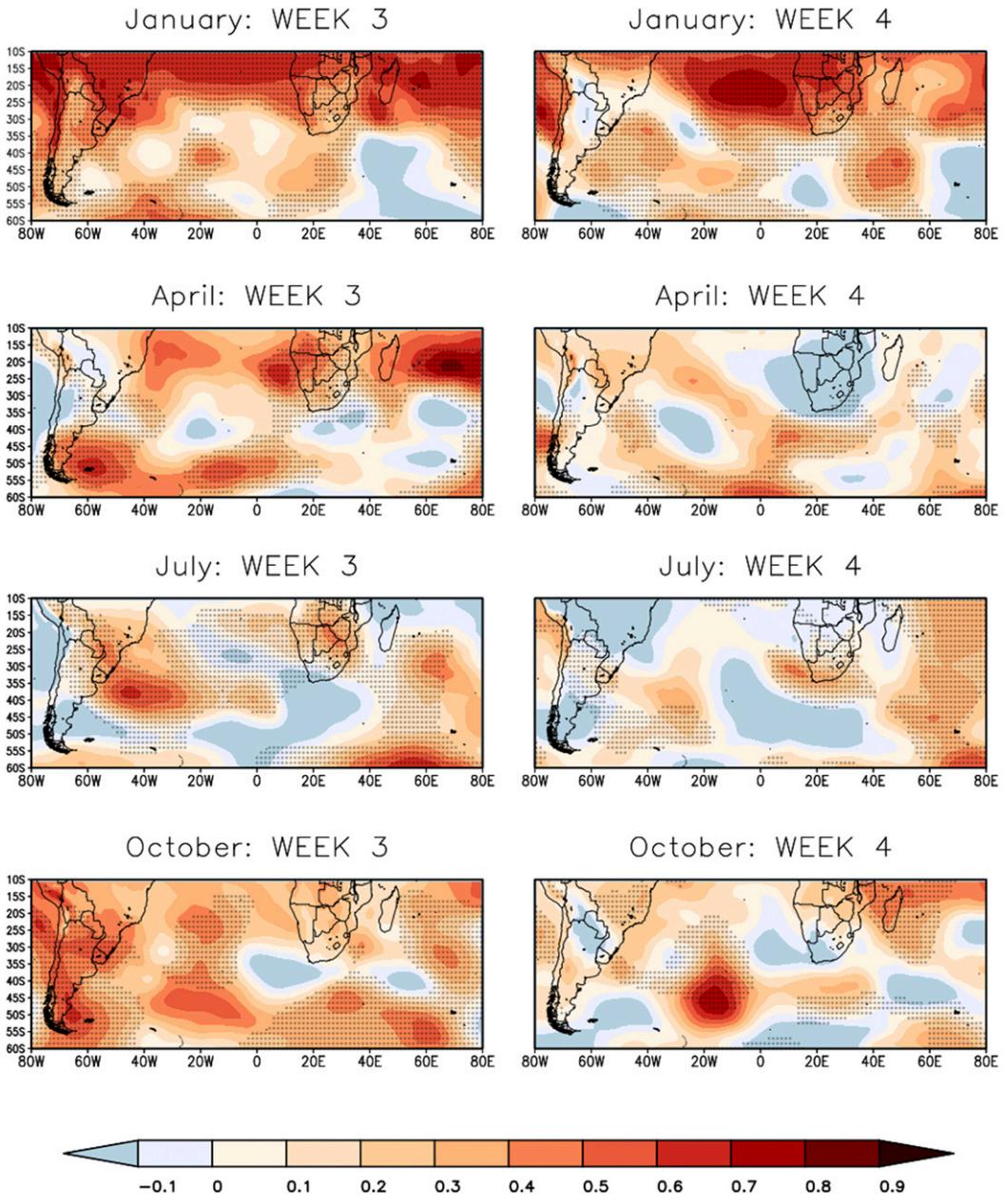

FIG. 5. Weekly mean 850-hPa geopotential height correlation between ECMWF forecasts and ERA-Interim for lead time in days corresponding to weeks 3 and 4 for January, April, July, and October. Crosses indicate where the forecasts outscore the persistence forecast.

are largely derived from initial conditions as opposed to lower boundary forcing from the tropical Pacific Ocean.

4. Conclusions

The NCEP CFSv2 and ECMWF hindcasts of 850-hPa geopotential heights from the S2S database were used to assess the subseasonal deterministic prediction skill of low-level circulation that affect southern Africa. The two hindcast systems, although verified across different periods and for a different number of start dates yielded broadly similar results in terms of the spatial patterns of skill for the week-3 and week-4 hindcasts. For a Southern Hemisphere domain containing the origin regions of weather systems impacting on southern Africa, the ACC shows skill relative to persistence into week 3 for some months. Generally, the hindcasts initialized in the warmer months have higher ACCs than the cold season hindcasts, with a clear separation in the ACCs between the warm and cold season hindcasts as the lead time increases. However, as this behavior of the ACCs with increasing lead

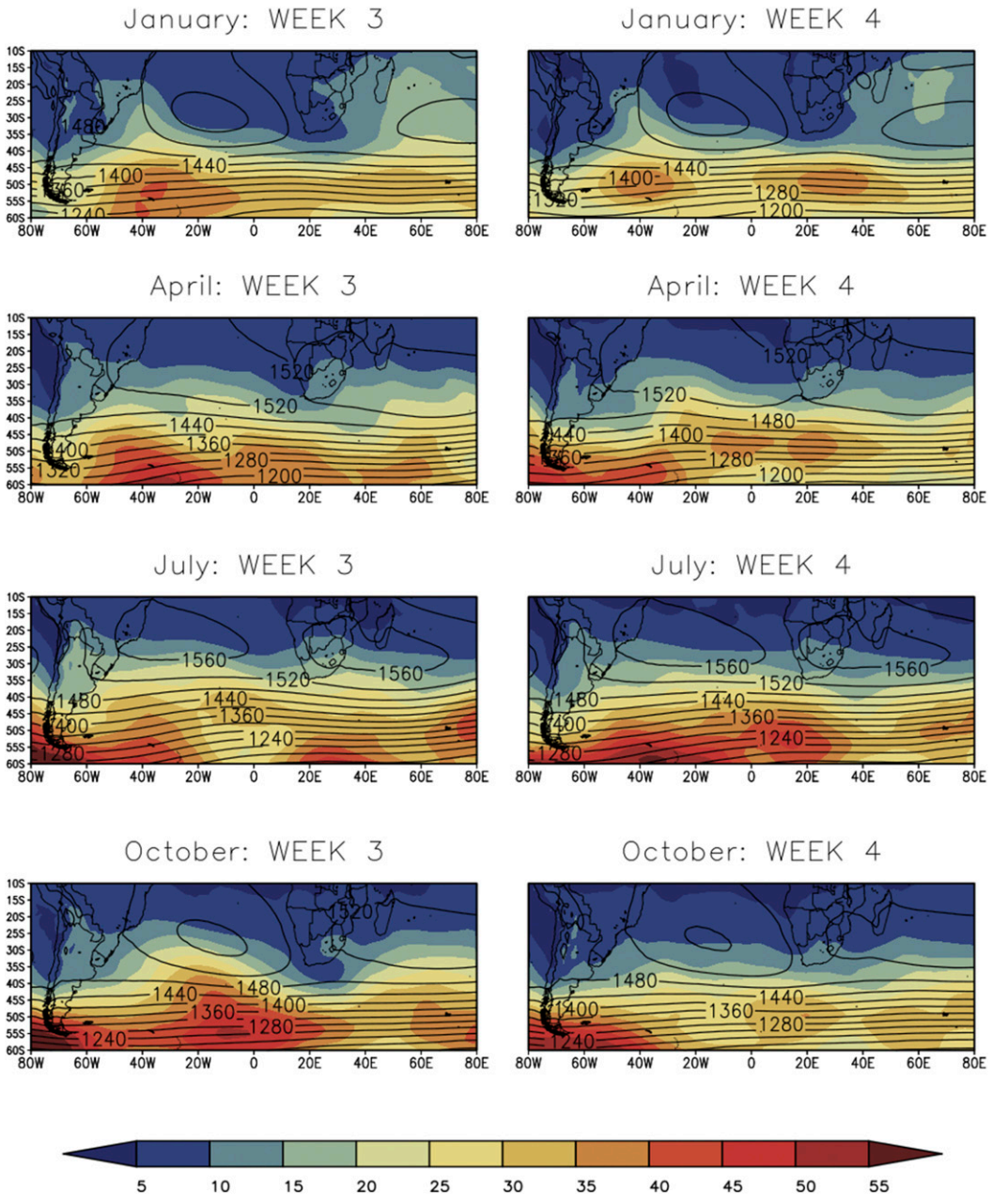

FIG. 6. ECMWF weekly mean climate of the 850-hPa geopotential height (contours) and the standard deviation (shaded colors) of the hindcasts corresponding to weeks 3 and 4 for January, April, July, and October.

time is also applicable to the persistence hindcasts, not all the warm month hindcasts are outscoring the cold month hindcasts in terms of the lead time reached before being beaten by persistence. There are variable spatial patterns of skill across the domain for the week-3 hindcasts and for all practical purposes no skill relative to persistence by week 4, except for some exceptions that will be mentioned where applicable in the discussion that follows.

For all the months prediction skill over persistence (indicated by the stippling on Figs. 3 and 5, Figs. S1 and S2) exists longest over South America, from where it often stretches eastward in a zonal band with a slight northwest–southeast orientation. This suggests strongly that information existing in atmospheric initial conditions over South America and the western Atlantic provides predictability as far out as weeks 3 and 4 of the forecasts. This occurs in particular during the predictions with start dates in the summer months. Interesting to note, is that the area over South America and the adjacent Atlantic Ocean where skill over persistence often peak, is in the vicinity of the South America monsoon and the South Atlantic convergence zone which are summer features as well as an area where low pressure systems occur relatively frequently (e.g., Taljaard 1967; Gozzo et al. 2014).

Another interesting feature to take note of, is the meridional bands where prediction skill of the modeling system outlasts that of persistence seen in some of the months. This feature usually occurs near the African subcontinent during the warmer months. This suggests that information existing in atmospheric ICs related to tropical temperate troughs and related cloud bands propagate southward in meridional bands providing predictability as far out as week 4 of the forecast.

The 2015–17 drought over the winter rainfall region of South Africa, with ''day zero'' indicative of the event where the City of Cape Town was to run out of water, has highlighted the need to be able to predict seasonal rainfall over the winter rainfall region of South Africa. However, this is a region with very limited predictability at the seasonal time scale in terms of both rainfall and the intraseasonal characteristics of rainfall. The results presented here show that from week 3, deterministic predictability of low-level circulation is for most of the winter months, an in particular the main rainfall months of June and July, not skillful relative to persistence over the areas where frontal troughs are expected to bring rainfall to the winter rainfall region of South Africa. However, the areas of skill relative to persistence over the central parts of South America that extend to the Atlantic Ocean, might provide an opportunity to extend the current predictability limit of low-level circulation on the subseasonal time scale. An association exist between anomalous convection over South America and the neighboring Atlantic region with rainfall over South Africa 4–5 days later, through a wave train that is generated by the anomalous convection that then impact regional circulation (Grimm and Reason 2015). This association exists throughout the year, although weaker for the winter and all-year rainfall region (east of the winter rainfall region along the southern coastal belt) compared to the summer rainfall region of South Africa. Interesting to note, is the skill relative to persistence in close proximity to the south and southeast of the subcontinent during the transitional seasons. Given that subseasonal predictability over some regions in South America has been shown to persist to week 3 for most months, and the presence of intraseasonal teleconnections between South America and South Africa, there exists the possibility of designing subseasonal rainfall predictions systems skillful for weeks 3 and 4 over southern Africa. Phakula et al. (2020) illustrated in a study that focused on the subseasonal prediction of minimum and maximum temperature over South Africa for the month of December, that skillful predictions are possible for the 11–30-day forecast over large parts of the country by application of a multimodel prediction system approach.

To summarize, the results are indicative of a potential of prediction skill for week 3 in terms of Southern Hemisphere circulation that impact on the southern African domain. Clear areas for further exploration include whether this skill translates to precipitation forecasts, the extent to which skill can be associated with certain synoptic types and weather regimes, and the use of probabilistic forecasts of both circulation and rainfall to exploit the deterministic skill that exists into week 3 and sometimes week 4 for various parts of the domain.

Acknowledgments. This work is supported by grants from the ACyS-ACCESS project funded by the NRF. The NCEP CFSv2 and ECMWF subseasonal forecast data used in this work are available from http://apps.ecmwf.int/datasets/data/s2s.

REFERENCES

Archer, E., W. Landman, J. Malherbe, M. Tadross, and S. Pretorius, 2019: South Africa's winter rainfall region drought: A region in transition? *Climate Risk Manage.*, **25**, 100188, https://doi.org/10.1016/j.crm.2019.100188.

Batté, L., C. Ardilouze, and M. Déqué, 2018: Forecasting West African heat waves at subseasonal and seasonal time scales. *Mon. Wea. Rev.*, **146**, 889–907, https://doi.org/10.1175/MWR-D-17-0211.1.

Blamey, R. C., and C. J. C. Reason, 2009: Numerical simulation of a mesoscale convective system over the east coast of South Africa. *Tellus*, **61A**, 17–34, https://doi.org/10.1111/j.1600-0870.2008.00366.x.

Dee, D. P., and Coauthors, 2011: The ERA-Interim reanalysis: Configuration and performance of the data assimilation system. *Quart. J. Roy. Meteor. Soc.*, **137**, 553–597, https://doi.org/10.1002/qj.828.

Driver, P., and C. J. C. Reason, 2017: Variability in the Botswana High and its relationships with rainfall and temperature characteristics over southern Africa. *Int. J. Climatol.*, **37**, 570–581, https://doi.org/10.1002/joc.5022.

Engelbrecht, C. J., 2017: Exploring subseasonal dynamic predictability of extreme events: A case study of the January and February heat waves. *33rd Annual Conf. of the South African Society for Atmospheric Sciences*, Polekwane, South Africa, South African Society for Atmospheric Sciences.

——, and W. A. Landman, 2016: Interannual variability of seasonal rainfall over the Cape south coast of South Africa and synoptic type association. *Climate Dyn.*, **47**, 295–313, https://doi.org/10.1007/s00382-015-2836-2.

——, ——, R. Graham, and P. McLean, 2017: Seasonal prediction skill of intraseasonal synoptic type variability over the Cape south coast of South Africa by making use of the Met Office Global Seasonal Forecast system 5. *Int. J. Climatol.*, **37**, 1998–2012, https://doi.org/10.1002/joc.4830.

Fauchereau, N., S. Trzaska, M. Rouault, and Y. Richard, 2003: Rainfall variability and changes in southern Africa during the 20th century in the global warming context. *Nat. Hazards*, **29**, 139–154, https://doi.org/10.1023/A:1023630924100.

Gozzo, L. F., R. P. Da Rocha, M. S. Reboita, and S. Sugahara, 2014: Subtropical cyclones over the southwestern South Atlantic: Climatological aspects and case study. *J. Climate*, **27**, 8543–8562, https://doi.org/10.1175/JCLI-D-14-00149.1.

Grimm, A. M., and C. J. C. Reason, 2015: Intraseasonal teleconnections between South America and South Africa. *J. Climate*, **28**, 9489–9497, https://doi.org/10.1175/JCLI-D-15-0116.1.

Hart, N. C. G., C. J. C. Reason, and N. Fauchereau, 2010: Tropical–extratropical interactions over southern Africa: Three cases of heavy summer season rainfall. *Mon. Wea. Rev.*, **138**, 2608–2623, https://doi.org/10.1175/2010MWR3070.1.

Joubert, A. M., S. J. Mason, and J. S. Galpin, 1996: Droughts over southern Africa in a doubled-CO_2 climate. *Int. J. Climatol.*, **16**, 1149–1156, https://doi.org/10.1002/(SICI)1097-0088(199610)16:10<1149::AID-JOC70>3.0.CO;2-V.

Kraaij, T., J. A. Baard, J. Arndt, L. Vhengani, and B. W. van Wilgen, 2018: An assessment of climate, weather, and fuel

factors influencing a large, destructive wildfire in the Knysna region, South Africa. *Fire Ecol.*, **14**, 4, https://doi.org/10.1186/s42408-018-0001-0.

Landman, W. A., and L. Goddard, 2002: Statistical recalibration of GCM forecasts over southern Africa using model output statistics. *J. Climate*, **15**, 2038–2055, https://doi.org/10.1175/1520-0442(2002)015<2038:SROGFO>2.0.CO;2.

——, and A. Beraki, 2012: Multi-model forecast skill for mid-summer rainfall over southern Africa. *Int. J. Climatol.*, **32**, 303–314, https://doi.org/10.1002/joc.2273.

Lyon, B., 2009: Southern Africa summer drought and heat waves: Observations and coupled model behaviour. *J. Climate*, **22**, 6033–6046, https://doi.org/10.1175/2009JCLI3101.1.

Malherbe, J., F. A. Engelbrecht, W. A. Landman, and C. J. Engelbrecht, 2012: Tropical systems from the southwest Indian Ocean making landfall over the Limpopo River Basin, southern Africa: A historical perspective. *Int. J. Climatol.*, **32**, 1018–1032, https://doi.org/10.1002/joc.2320.

Mason, S., and M. Jury, 1997: Climatic variability and change over southern Africa: A reflection on underlying processes. *Prog. Phys. Geogr.*, **21**, 23–50, https://doi.org/10.1177/030913339702100103.

Mastrangelo, D., and P. Malguzzi, 2019: Verification of two years of CNR-ISAC subseasonal forecasts. *Wea. Forecasting*, **34**, 331–344, https://doi.org/10.1175/WAF-D-18-0091.1.

Mundhenk, B. D., E. A. Barnes, E. D. Maloney, and C. F. Baggett, 2018: Skillful empirical subseasonal prediction of landfalling atmospheric river activity using the Madden–Julian Oscillation and quasi-biennial oscillation. *Climatic Atmos. Sci.*, **1**, 20177, https://doi.org/10.1038/s41612-017-0008-2.

Osman, M., and M. S. Alvarez, 2018: Subseasonal prediction of the heat wave of December 2013 in southern South America by the POAMA and BCC-CPS models. *Climate Dyn.*, **50**, 67–81, https://doi.org/10.1007/s00382-017-3582-4.

Pascale, S., B. Pohl, S. B. Kapnick, and H. Zhang, 2019: On the Angola low interannual variability and its role in modulating ENSO effects in southern Africa. *J. Climate*, **32**, 4783–4803, https://doi.org/10.1175/JCLI-D-18-0745.1.

Phakula, S., W. A. Landman, and A. Beraki, 2018: Forecasting seasonal rainfall characteristics and onset months over South Africa. *Int. J. Climatol.*, **38**, e889–e900, https://doi.org/10.1002/joc.5417.

——, ——, C. J. Engelbrecht, and T. Makgoale, 2020: Forecast skill of minimum and maximum temperatures on subseasonal timescales over South Africa. *Earth Space Sci.*, **7**, e2019EA000697, https://doi.org/10.1029/2019EA000697.

Reason, C. J. C., and A. Keibel, 2004: Tropical Cyclone Eline and its unusual penetration and impacts over the southern African mainland. *Wea. Forecasting*, **19**, 789–805, https://doi.org/10.1175/1520-0434(2004)019<0789:TCEAIU>2.0.CO;2.

——, and M. Rouault, 2005: Links between the Antarctic Oscillation and winter rainfall over western South Africa. *Geophys. Res. Lett.*, **32**, L07705, https://doi.org/10.1029/2005GL022419.

Rouault, M., and Y. Richard, 2005: Intensity and spatial extent of droughts in southern Africa. *Geophys. Res. Lett.*, **32**, L15702, https://doi.org/10.1029/2005GL022436.

Saha, S., and Coauthors, 2014: The NCEP Climate Forecast System version 2. *J. Climate*, **27**, 2185–2208, https://doi.org/10.1175/JCLI-D-12-00823.1.

Seo, E., and Coauthors, 2019: Impact of soil moisture initialization on boreal summer subseasonal forecasts: Mid-latitude surface air temperature and heat wave events. *Climate Dyn.*, **52**, 1695–1709, https://doi.org/10.1007/s00382-018-4221-4.

Simmonds, I., and K. Keay, 2000: Mean Southern Hemisphere extratropical cyclone behavior in the 40-Year NCEP–NCAR Reanalysis. *J. Climate*, **13**, 873–885, https://doi.org/10.1175/1520-0442(2000)013<0873:MSHECB>2.0.CO;2.

Singleton, A. T., and C. J. C. Reason, 2007: A numerical model study of an intense cutoff low pressure system over South Africa. *Mon. Wea. Rev.*, **135**, 1128–1150, https://doi.org/10.1175/MWR3311.1.

Sousa, P. M., R. C. Blamey, C. J. C. Reason, A. M. Ramos, and R. M. Trigo, 2018: The 'day zero' Cape Town drought and the poleward migration of moisture corridors. *Environ. Res. Lett.*, **13**, 124025, https://doi.org/10.1088/1748-9326/aaebc7.

Taljaard, J. J., 1967: Development, distribution and movement of cyclones and anticyclones in the Southern Hemisphere during the IGY. *J. Appl. Meteor.*, **6**, 973–987, https://doi.org/10.1175/1520-0450(1967)006<0973:DDAMOC>2.0.CO;2.

Tian, D., E. F. Wood, and X. Yuan, 2017: CFSv2-based sub-seasonal precipitation and temperature forecast skill over the contiguous United States. *Hydrol. Earth Syst. Sci.*, **21**, 1477–1490, https://doi.org/10.5194/hess-21-1477-2017.

Vitart, F., and Coauthors, 2017: The Subseasonal to Seasonal (S2S) prediction project database. *Bull. Amer. Meteor. Soc.*, **98**, 163–173, https://doi.org/10.1175/BAMS-D-16-0017.1.

White, C. J., D. Hudson, and O. Alves, 2014: ENSO, the IOD and the intraseasonal prediction of heat extremes across Australia using POAMA-2. *Climate Dyn.*, **43**, 1791–1810, https://doi.org/10.1007/s00382-013-2007-2.

——, and Coauthors, 2017: Potential applications of subseasonal-to-seasonal (S2S) predictions. *Meteor. Appl.*, **24**, 315–325, https://doi.org/10.1002/met.1654.